Design and Performance of a 215 GHz Pulsed Radar System

ROBERT E. McINTOSH, FELLOW, IEEE, RAM M. NARAYANAN, STUDENT MEMBER, IEEE, JAMES B. MEAD, STUDENT MEMBER, IEEE, AND DANIEL H. SCHAUBERT, SENIOR MEMBER, IEEE

Abstract—**The advent of high-power extended interaction oscillators and low-noise receivers in the 215 GHz frequency window has made it possible to design and operate radar systems at these wavelengths. This paper describes a high-power 215 GHz pulsed radar system developed for remote sensing applications that is capable of making backscatter measurements from terrain targets at ranges of several kilometers under normal atmospheric conditions. The paper also discusses system performance and calibration, together with measurements of snow backscatter coefficients made during early 1987.**

I. INTRODUCTION

THE RECENT availability of high-power sources operable in the 215 GHz absorption window combined with the advantage of high gain from small apertures makes this frequency band attractive for the development of radar systems. Although atmospheric absorption ultimately limits long-range sensing, applications in the 0–5 km range are currently possible with apertures having diameters under 0.25 m. Range is limited by water vapor attenuation, which may vary between 1 $dB \cdot km^{-1}$ under cold, dry conditions to as much as 12 $dB \cdot km^{-1}$ under hot, humid conditions, and by rain attenuation, which may vary between 1 $dB \cdot km^{-1}$ in light rain to over 30 $dB \cdot km^{-1}$ in a heavy downpour [1]. Therefore, it is difficult to design a system that guarantees target detection beyond a few km for all possible conditions. Maximum range for dry desert or arctic environments might conceivably be extended to more than 20 km with antenna sizes below 1 m in diameter.

Fig. 1 shows calculations of absorption due to oxygen, water vapor, and rain as a function of frequency [2]. Above 100 GHz, absorption due to rain is only weakly dependent on frequency. Conversely, absorption due to water vapor is strongly dependent on frequency, having well-defined peaks near 22 and 183 GHz. Skirts of these lines as well as others above 300 GHz cause appreciable attenuation at 215 GHz.

The development of near-millimeter-wave vacuum tube sources capable of tens of watts of pulsed power along with the availability of solid-state LO sources and efficient mixers has made it practical to build prototype radar systems operating at 215 GHz. One such radar system, developed recently by the University of Massachusetts (UMass), is the subject of this paper. This incoherent system utilizes an extended interaction oscillator (EIO) to transmit 60 W of peak pulse power and is used for remote sensing studies. Results given in this paper show that this system can measure terrain clutter at ranges up to several km.

The UMass 215 GHz radar system is described in Section II. Details of the transmitter, receiver, antennas, and control/data acquisition subsystems are given. The operation of the overall system is discussed in Section III, including considerations of propagation effects, system calibration, and achievable range performance. We conclude the paper by presenting backscatter coefficient measurements of snow in Section IV, which we believe are the first ever made in this frequency range.

II. SYSTEM DESCRIPTION

A block diagram of the UMass 215 GHz radar system is given in Fig. 2, which shows major subsystem interconnections, and its performance characteristics are summarized in Table I. The radar system uses a Varian VKY2429M1 EIO to transmit 60 W, 100 ns duration pulses. Pulse repetition frequencies between 700 Hz and 20 kHz can be externally controlled in 100 Hz steps using a specially designed radar control and data acquisition (RACDA) subsystem. The receiver front end consists of a single-ended mixer driven by a 71.2 GHz InP Gunn diode local oscillator through a frequency tripler. The double sideband (DSB) noise figure of this mixer subsystem is 10 dB. An automatic frequency control (AFC) loop operating between 1.2 and 1.6 GHz down-converts the signal to 160 MHz, where a logarithmic amplifier is used for detection. Separate 6 in. Gaussian optics lens antennas with scalar feed horns are used to achieve high isolation between transmitter and receiver without the use of a circulator and/or T/R switch. The transmitter and receiver are enclosed in two separate boxes of square cross section that can be rotated so that a complete set of polarization combinations may be measured. Having separate transmitter and receiver modules also allows bistatic measurement capability. The transmitter and receiver modules with lens antennas attached can be seen in the photograph of Fig. 3

Manuscript received August 7, 1987; revised January 22, 1988. This work was supported by the U.S. Army Research Office under Contract DAAG29-85-K-0227.

The authors are with the Department of Electrical and Computer Engineering, University of Massachusetts, Amherst, MA 01003.

IEEE Log Number 8821066.

0018-9480/88/0600-0994$01.00

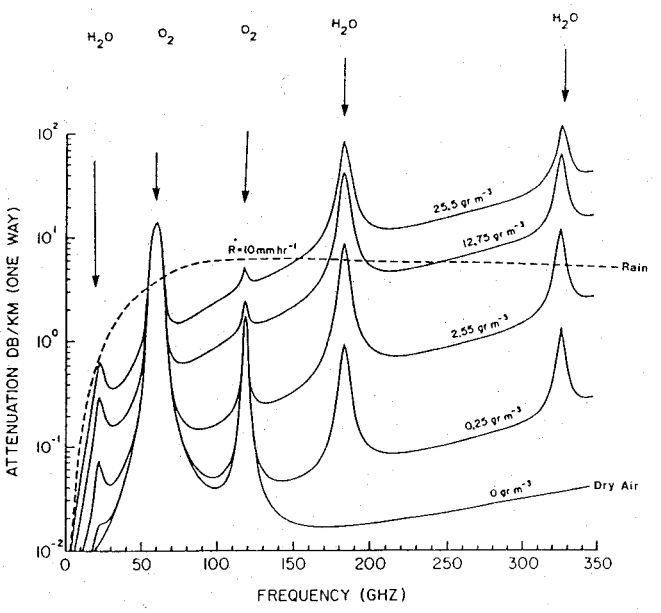

Fig. 1. Sea-level absorption spectrum due to atmospheric gases for various humidity conditions. Included is attenuation due to rain at 10 mm·hr^{-1} rain rate.

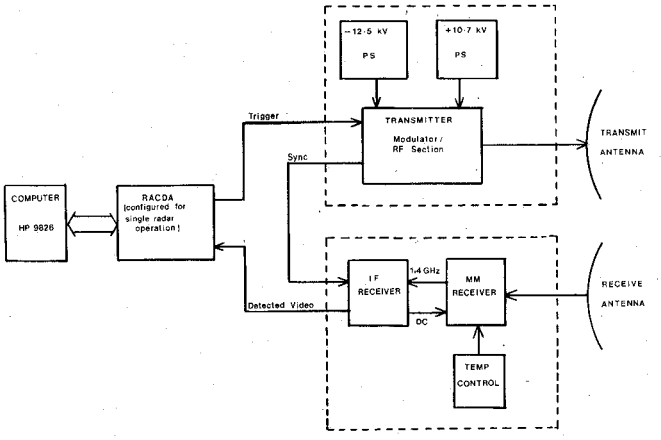

Fig. 2. Interconnection diagram of 215 GHz radar.

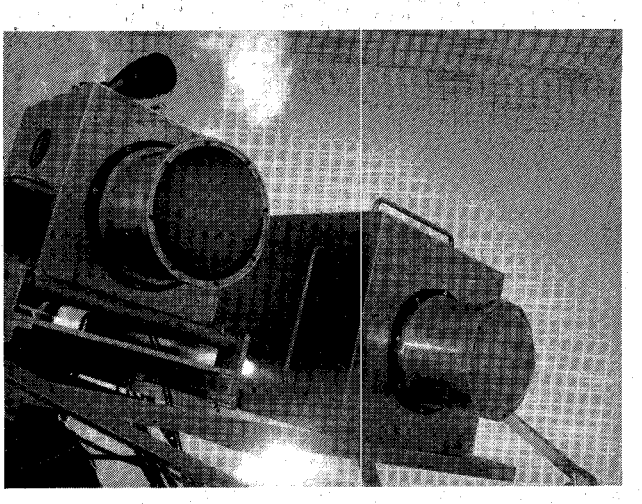

Fig. 3. Photograph of the 215 GHz radar system showing various major components. The receiver with its sighting scope is on the left, while the transmitter is on the right. The two lens antennas can also be seen.

TABLE I
CHARACTERISTICS OF UMASS 215 GHZ RADAR SYSTEM

Transmitter		
Center Frequency	215 GHz Nominal	
Peak Output Power	60W	
Pulsewidth	100 nsec	
PRF	2/10 KHz Internal	
	700 Hz – 20 KHz External	
Tuning Bandwidth	300 MHz	
Antennas		
	Lens	Horn
3 dB beamwidth	0.64 deg	23 deg
Directivity	49.6 dB	18.5 dB
Receiver		
Noise Figure	10 dB DSB	
1st IF	1.4 GHz	
2nd IF	160 MHz	
Bandwidth	300 MHz, 1st IF	
	40 MHz, 2nd IF	
Dynamic Range	70 dB	
System		
Polarization	Linear HH, HV, VH, VV	
Operating Mode	Monostatic or Bistatic	
Positioning	Azimuth and Elevation	

A. Transmitter

A block diagram of the transmitter is shown in Fig. 4. The design is based on a 215 GHz transceiver system originally developed by Norden Systems for the U.S. Army Night Vision and Electro-Optics Laboratory. The transmitter contains high-voltage power supplies, a modulator, and an EIO manufactured by Varian.

The EIO is a klystron-like vacuum tube containing a single resonator cavity which houses a ladder structure through which an electron beam passes [3]. Large RF fields are developed in the gaps between the rungs. The EIO has three electrodes: a cathode, an anode, and a collector, which is grounded to the outer casing. In the resting state, the anode and cathode are biased 12.5 kV below the collector. The cathode is then pulsed an additional 9.2 kV below the anode, causing the tube to conduct. This accelerating potential is adjusted to obtain the proper beam velocity for oscillations to occur. The EIO can be electronically tuned in a 300 MHz range about its nominal operating frequency of 215 GHz. Peak output power of approximately 60 W was measured using a Thompson calorimeter.

The modulator consists of an internal PRF Generator, an FET switch, and a high-voltage triode switch. The PRF Generator utilizes an SN555 timing circuit to obtain PRF's of 2 or 10 kHz. This timing circuit triggers a monostable circuit, which establishes the time duration of the transmit pulse. The monostable circuit can also be externally triggered by the RACDA subsystem to generate PRF's from

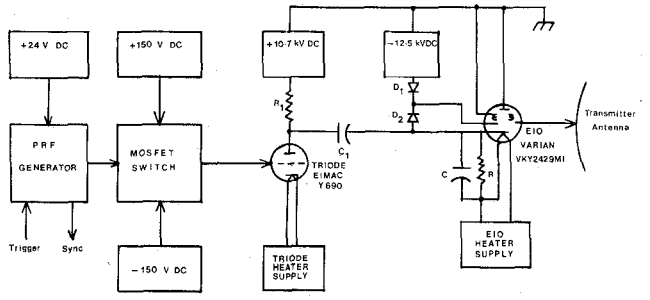

Fig. 4. Block diagram of radar transmitter.

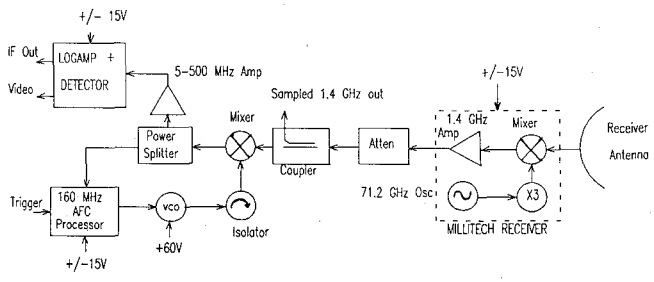

Fig. 6. Block diagram of radar receiver.

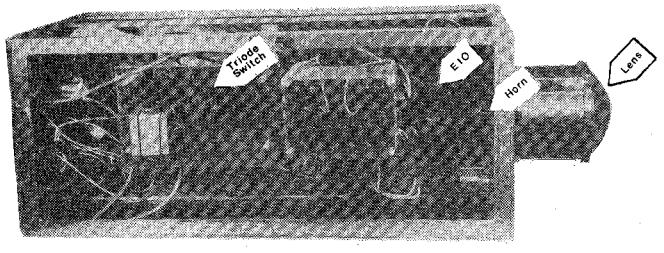

Fig. 5. View of radar transmitter showing the EIO and modulator. The corrugated horn and lens antenna are also shown.

700 Hz to 20 kHz in 100 Hz steps. The output of this low-power driver is transformer coupled to a Siliconix IRF441 MOSFET switch. This FET was selected for its high peak current capability in order to handle the 10 A pulse transferred through the FET to the grid of a planar ceramic EIMAC Y690 triode switch tube. When the pulse is off, the triode grid is clamped at -150 V, to ensure cutoff. When the pulse is on, this voltage rises to $+60$ V, thus driving the tube into saturation. A microfuse (0.2 A) in the FET drain circuit protects the triode from accidental short circuit and prevents the application of a continuous positive voltage to its grid.

The triode switch acts as a hard-tube modulator, which is capable of providing the high peak currents to rapidly charge the EIO stray capacitance, while simultaneously providing a flat pulse to minimize EIO frequency drift. When the pulse is off, the triode anode voltage is $+10.7$ kV but it drops to $+1.5$ kV when the triode is switched on. This negative 9.2 kV pulse is capacitively coupled to the EIO cathode, causing the EIO to oscillate. Fig. 5 shows an inside view of the transmitter.

B. Receiver

The block diagram of the receiver is shown in Fig. 6. The receiver consists of two units: the millimeter-wave receiver (shown within dotted lines) and the IF receiver. The mixer, the local oscillator, and the 1.4 GHz IF amplifier were fabricated by Millitech, Inc., as an integrated package for improved reliability and minimized losses. A GaAs Schottky barrier diode allows the mixer to operate with -10 dBm of LO drive. The LO consists of a fixed-tuned 71.2 GHz InP Gunn oscillator, which offers higher power, improved dc-to-RF efficiency, and lower noise than GaAs Gunn oscillators. A GaAs varactor diode tripler provides approximately 0 dBm of LO power at 215 GHz. This is injected into the signal path via a 10 dB coupler. The 1.4 GHz IF preamplifier, with a gain of 37.4 dB and a noise figure of 1 dB, is connected directly to the mixer in order to minimize cable losses. Overall RF-to-IF gain of the receiver front end is 26 dB, with a DSB noise figure of 9.3 dB. To minimize thermal frequency drifts, the multiplier temperature is stabilized at $30° \pm 2°$C for ambient temperatures ranging between $-10°$ and 35°C.

The output of the millimeter-wave receiver at 1.4 GHz is further down-converted to a second IF of 160 MHz using a termination-insensitive mixer with a conversion loss of 6.5 ± 0.7 dB over a wide range of RF/LO frequencies and termination mismatches. A 3 dB power splitter directs one half of this signal into a pulsed AFC processor, which provides the tuning voltage to the 1–2 GHz VCO to correct for long-term frequency drifts in the system. The second output from the 3 dB power splitter is amplified by a 17.5 dB gain wide-band (5–500 MHz) amplifier, prior to detection by the logarithmic amplifier. The log amp provides a transfer function of approximately 26 mV/dB over a dynamic range of 70 dB (0 to -70 dBm). By operating at 160 MHz, a video bandwidth of 40 MHz is available to detect received pulses as narrow as 25 ns. The detected video output of the log amp/detector is fed to RACDA for further processing. Fig. 7 shows the millimeter-wave and the IF receivers.

C. Antennas

Two separate antennas are used for the transmitter and receiver. This configuration permits separate transmitter and receiver polarization options, bistatic capability, and transmission measurements. Each of the antennas consists of a 6 in. diameter Gaussian optics lens illuminated by a corrugated scalar feed horn connected directly to the transmitter and receiver. The Gaussian optics lens antennas form well-defined Gaussian beams through the use of corrugated horns and matched dielectric lenses [4]. Their radiation patterns are characterized by circular symmetry, high efficiency, and low sidelobes. The antennas have 3 dB beamwidths of 0.64°, directivities of 49.6 dB, and sidelobes of -25 dB or less. The horn antennas feeding the lenses have 3 dB beamwidths of 23°, directivities of 18.5 dB, and

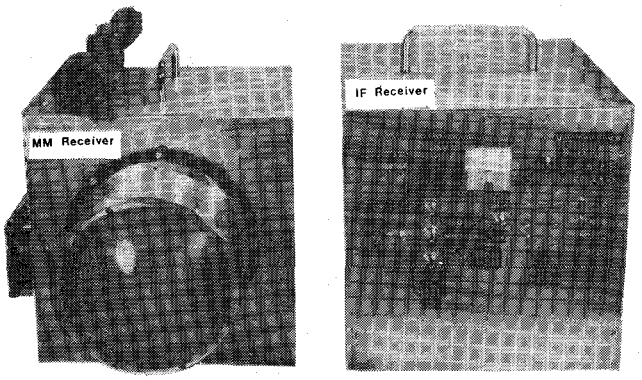

Fig. 7. Photograph of millimeter-wave and IF receivers.

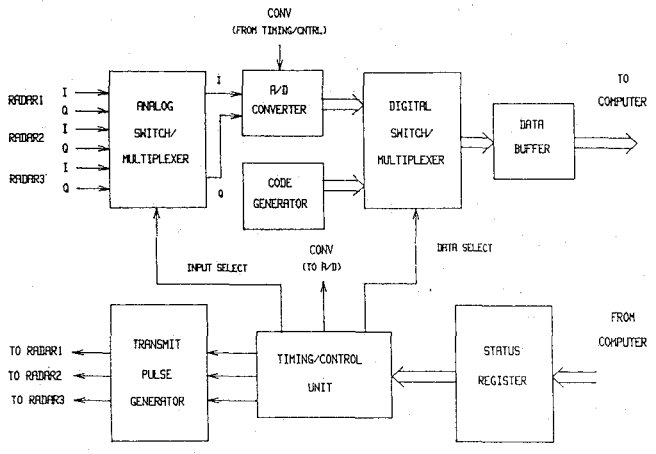

Fig. 8. Block diagram of radar control and data acquisition (RACDA) subsystem.

sidelobes less than −27 dB. The system can be operated with or without the lenses, depending on the application. The performance curves and measurements indicated in this paper relate to both lenses being used in the system.

D. Radar Control and Data Acquisition Subsystem

A block diagram of the RACDA subsystem is shown in Fig. 8. This specially designed subsystem was developed to simultaneously control and gather measurement data from multiple radar systems. Video I and Q channel signals from three different coherent radars can be time-multiplexed and digitized with this subsystem. Timing/control units generate the system timing and control signals to sequentially trigger three pulsed radar transmitters, and process the return video pulses from the corresponding receivers. Backscattered signals from distributed targets can be profiled with range resolutions of 15 m, corresponding to transmit pulse widths of 100 ns. User interface is achieved through an HP9826 Hewlett-Packard desktop computer and an HP6944A multiprogrammer. User-interactive software has been developed that facilitates the control of the radars and the formatting of measured radar data.

The user may sample up to 15 adjacent range gates with a minimum range of 50 m to a maximum of 150 000/(n·PRF) km, where n is the number of radars being controlled. The return signals are quantized by high-speed flash 8-bit A/D converters into 256 levels corresponding to a resolution of 0.3 dB, and a 1/2 least significant bit (LSB) quantization error of 0.15 dB. In addition, the RACDA subsystem can store up to 64K words for continuous data acquisition operation. In these measurements, the RACDA subsystem was configured for single radar operation.

III. Performance Considerations

A. Atmospheric Propagation Effects

The performance of the 215 GHz radar is limited by water vapor as well as hydrometeors, such as rain, fog, and snow. Dry air attenuation is negligible, having a value of about 0.02 dB/km at sea level at 15°C. Improved algorithms have been developed [5] to predict water vapor attenuation at high water vapor densities. A simplified expression for the specific attenuation, γ_w (in dB·km^{-1}) at 215 GHz is given by

$$\gamma_w = 0.2833\rho + 9.71\times10^{-3}\rho^2 \qquad (1)$$

where ρ is the water vapor density in g·m^{-3} and the temperature is assumed to be 15°C. A temperature dependence of −0.7 percent/°C (−0.03 dB/°C) can be applied at temperatures other than 15°C. A more accurate model, presented by Liebe [1], includes the contribution of all resonance lines in the millimeter-wave spectrum.

Few data exist for attenuation of 215 GHz signals through rain. Data taken by Bauerle at U.S. Army Ballistic Research Laboratory (BRL) [6] at 217 GHz suggest an exponential type of relation between specific attenuation in dB·km^{-1} and rain rate in mm·hr^{-1}. Abridged tables are also available [7], which permit interpolation based on which the specific attenuation due to rain, γ_r (in dB·km^{-1}), may be approximated to within 15 percent by

$$\gamma_r = 2r^{2/3} \qquad (2)$$

where r is the rain rate in mm·hr^{-1}. The above relation is valid at 20°C and varies less than 1 percent for temperatures ranging from 0 to 40°C. The above tables use Mie scattering computations with Marshall–Palmer drop size distribution.

B. Calibration

Precision millimeter-wave trihedral corner reflectors of internal edge dimension 1.5 in. and 3 in. are used to externally calibrate the radar system during measurements. The corner reflectors were made of 0.375 in. aluminum cast machined plate lapped to a surface flatness of ±0.0002 in. and a surface finish of 15 μ in. The sides were perpendicular to within 0.0125° per 6 in. The maximum theoretical radar cross section, occurring along the axis of

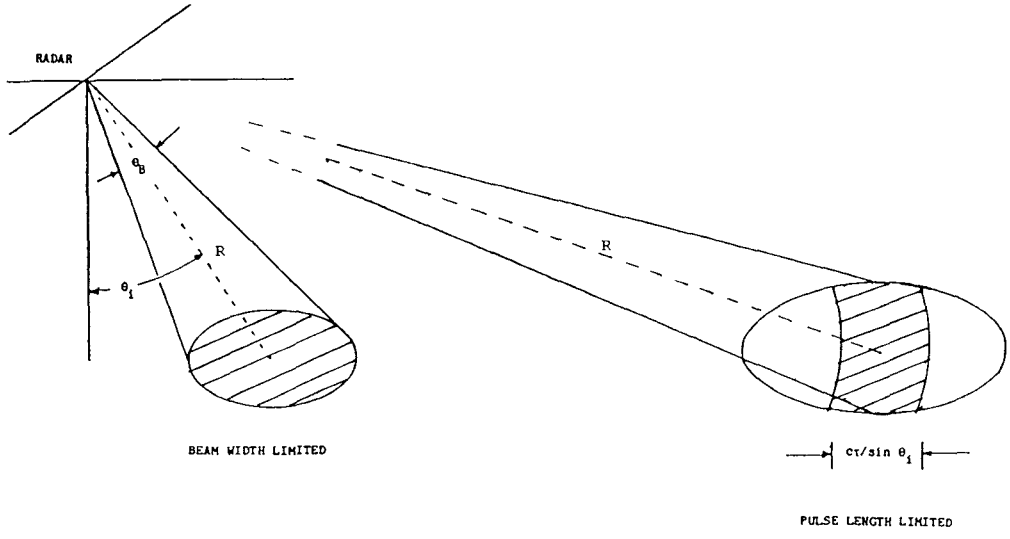

$$\tan\theta_i < \frac{c\tau}{2\theta_B R} \qquad \tan\theta_i > \frac{c\tau}{2\theta_B R}$$

Fig. 9. Antenna beam geometry.

symmetry, is given by [8]

$$\sigma = \frac{4\pi l^4}{3\lambda^2} \tag{3}$$

where l is the length of one of the internal edges.

The radar cross sections are computed as 4.533 m^2 for $l = 1.5$ in. and 72.53 m^2 for $l = 3$ in.

The corner reflector is mounted on a 20 ft mast of small diameter pipe and located in a flat area free of interfering targets. Five hundred return pulses are averaged at a time to obtain the mean return power. Temperature and humidity measurements are made simultaneously to eliminate the effect of atmospheric attenuation by estimating propagation path losses between the radar and the target area under consideration.

C. Range Performance

The power of a radar signal reflected from a natural surface lying within the antenna footprint, shown in Fig. 9, is given for the beamwidth-limited case by

$$P_r \cong \frac{P_t G^2 \theta_B^2 \sigma^0 \lambda_0^2 L_{TR} e^{-2(\gamma_w+\gamma_r)R}}{16(4\pi)^2 R^2 \cos\theta_i (2ln2)}, \qquad \tan\theta_i < \frac{c\tau}{2\theta_B R} \tag{4a}$$

and for the pulse width limited case by

$$Pr \cong \frac{P_t G^2 \theta_B \sigma^0 c\tau \lambda_0^2 L_{TR} e^{-2(\gamma_w+\gamma_r)R}}{128\pi^3 R^3 \sin\theta_i (2ln2)}, \qquad \tan\theta_i > \frac{c\tau}{2\theta_B R} \tag{4b}$$

where γ_w and γ_r are expressed in nepers$\cdot m^{-1}$ [9]. For the UMass 215 GHz radar, we have the transmitted pulse power $P_t = 60$ W; the estimated antenna gain $G_T = G_R = G \approx 48.6$ dB (assume antenna efficiency ≈ 80 percent); the antenna beamwidth, $\theta_B = 0.01117$ rad; the wavelength $\lambda_0 = 1.395 \times 10^{-3}$ m; the speed of light $c = 3 \times 10^8$ m$\cdot s^{-1}$; and the transmitted pulse width $\tau = 100$ ns. The distance to the center of the target area is denoted by R, and the angle of incidence by θ_i. σ^0 denotes the normalized radar cross section (NRCS) or the average backscatter coefficient, viz., the radar cross section per unit area, of the natural surface. We assume 2 dB of losses in the transmitter and receiver; hence $L_{TR} = 0.63$. The factor $2ln2$ appearing in the denominator is used to account for nonuniform antenna gain across the beam footprint and assumes a Gaussian antenna pattern [10], which is a good approximation in our case. The noise floor at the input of the receiver is computed as -84.8 dBm at 27°C, corresponding to an SSB noise figure of 13 dB. We solve (4a) and (4b) to obtain an expression for the maximum range, R_{max}, of the radar system for an SNR of unity, as a function of $(\sigma^0/\cos\theta_i)$. Solutions of the above expression are plotted in Fig. 10(a) and (b) for various relative humidities at 20°C (we assume $\gamma_r = 0$) for the beamwidth and the pulse length limited case, respectively. The abscissa in both plots is $10\cdot\log(\sigma^0/\cos\theta_i)$ in dB.

The curves in Fig. 10 are derived for the detection of single pulses and are somewhat optimistic because they do not include other effects that limit the range performance of a radar. However, the maximum range of the UMass 215 GHz radar is enhanced by the RACDA subsystem's ability to integrate numerous pulses to reduce the effects of system noise. SNR improvement is approximately $\sqrt{N}$, where N is the number of pulses integrated.

Also shown in Fig. 10(a) is the experimental range value that has been realized by integrating 1000 return pulses. The radar was pointed at a wet snow field of average NRCS of -15 dB on a warm day with a temperature of 20°C and a 35 percent relative humidity. The range to the target, R, was 120 m and the local incidence angle, θ_i, was 70.5°. The beamwidth-limited expression is applicable to this case. The mean SNR measured was 33.5 dB, and this point is shown as A in the figure. We have also projected this measured range up by a ratio of 47.3 ($10\log 47.3^2 = 33.5$

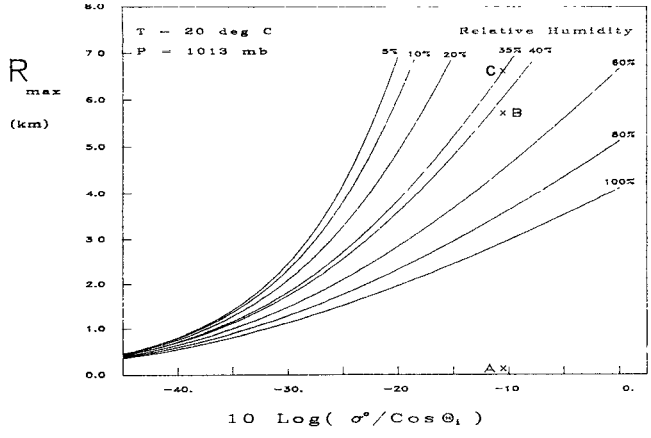

(a)

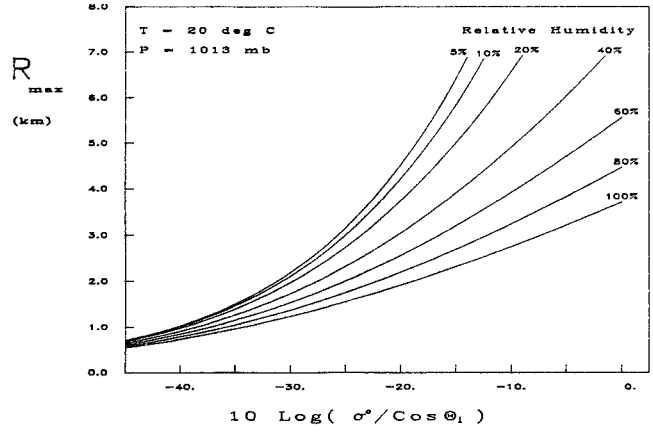

(b)

Fig. 10. R_{max} versus $10\cdot\log(\sigma^0/\cos\theta_i)$ for various relative humidity values for (a) beamwidth-limited case and (b) pulse-length-limited case. Point *B* denotes experimentally measured value, normalized to SNR = 1.

dB) to the point marked *B* in order to normalize it to an SNR of 1 for comparison with the theoretical curve. It is seen that the experimentally measured range of 5.7 km agrees closely with the theoretical value of approximately 6.6 km, shown as *C*.

D. System Stability

Stability of the overall system gain is necessary when making accurate radar cross section measurements. Short-term gain stability of better than 1.0 dB has been achieved during the data acquisition process by the following steps: (1) operating the hard-tube modulator in the saturated mode, thereby minimizing frequency variations and power fluctuations caused by variations in the EIO cathode voltage, and (2) temperature stabilization of the millimeter-wave receiver to minimize frequency and gain variations. AFC on a pulse-to-pulse basis also serves to maintain the second IF at 160 ± 3 MHz, well within the flat transfer characteristic of the log amp/detector. Fig. 11 shows a typical plot of received power from the 3 in. corner reflector at a range of 480 m sampled 500 times during a measurement.

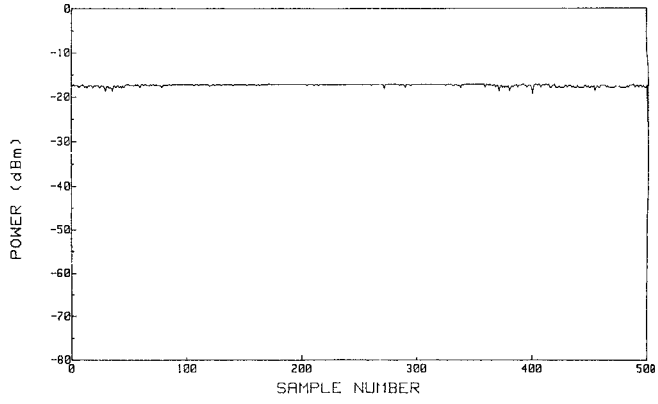

Fig. 11. Return from 3 in. corner reflector as recorded by RACDA, at input to IF receiver.

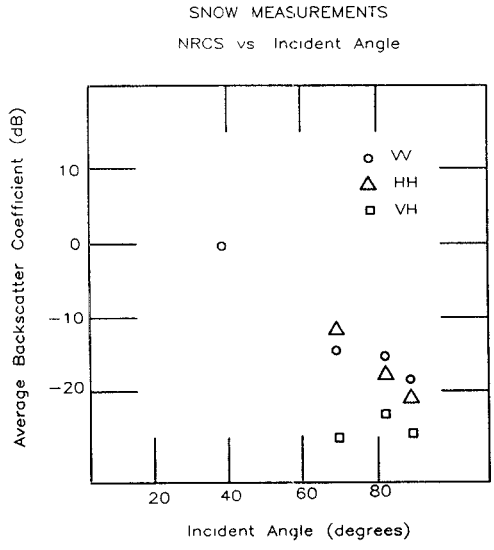

θ_i	Date	Site	Range	Snow Conditions	# Points Averaged
39°	Feb 4/5 average	UMass	105m	Dry Snow	19
70.5°	Mar 24	E Corinth Vermont	120m	Wet Snow	104–VV 26–VH/HH
83 2°	Mar 11	UMass	800m	Dry Frozen Snow	21
86.5°	Mar 11	UMass	1500m	Dry Frozen Snow	21

Fig. 12. NRCS of snow measured at various incidence angles, under conditions indicated.

IV. Normalized Radar Cross Section Measurements

Preliminary measurements of the average backscatter coefficients of snow were made at incidence angles of 39°, 70.5°, 83.2°, and 86.5° during February and March, 1987. The data are plotted in Fig. 12. These measurements are of interest because of the relatively high clutter that snow can contribute to radar and communication signals.

To obtain a sufficient number of statistically independent samples of the radar return signals, a large number of measurements were made at each incidence angle by mov-

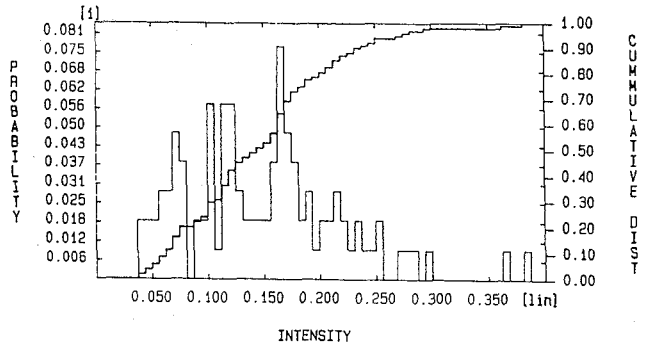

Fig. 13. Histogram of square-root of return power from snow at $\theta_i = 70.5°$, VV, 104 points.

ing either the position of the antenna footprint by one antenna beamwidth or the position of the radar antennas by one antenna diameter. A histogram of the square root of the return power showing the statistics of 104 vertical transmit–vertical receive (VV) data points obtained at 70.5° incidence angle is shown in Fig. 13. Calculations of the mean value, standard deviation, skewness, and kurtosis indicate that the amplitude of the scattered returns is Rayleigh distributed. Measurements made at other grazing angles also indicate that Rayleigh fading occurs in all of our snow backscatter measurements. This information should be helpful for radar designers concerned with optimal systems capable of good clutter rejection performance.

V. Conclusions

A 215 GHz radar capable of making scattering measurements up to several km range has been described. By using separate transmit and receive antennas, the amplitudes of the polarization matrix elements may be measured conveniently. A dedicated data acquisition system was developed allowing up to 15 range gates to be sampled at 100 ns intervals. Instrument stability of ± 1.0 dB yields accurate scattering measurements of a variety of terrestrial targets. This paper demonstrates that a portable, high-resolution millimeter-wave radar capable of target detection up to several km is achievable using current technology. Comprehensive backscatter coefficient measurements are planned, the results of which will be published when available.

Acknowledgment

The authors are grateful to Dr. C. Swift of the University of Massachusetts, Dr. W. Flood of the U.S. Army Research Office, R. Mastroianni of Norden Systems and R. Chedester of Millitech Corporation for helpful discussions and suggestions, and to Y. F. Chao and D. Vandemark of the University of Massachusetts for help with the measurements.

References

[1] H. J. Liebe, "An updated model for millimeter wave propagation in moist air," *Radio Sci.*, vol. 20, pp. 1069–1089, Sept.–Oct. 1985.

[2] R. Lhermitte, "A 94 GHz Doppler radar for cloud observations," *J. Atmos. Ocean. Tech.*, vol. 4, pp. 36–48, Mar. 1987.

[3] W. R. Day and J. A. Noland, "The millimeter-wave extended interaction oscillator," *Proc. IEEE*, vol. 54, pp. 539–543, Apr. 1966.

[4] P. F. Goldsmith, "Quasi-optical techniques at millimeter and submillimeter wavelengths," ch. 5 in *Infrared and Millimeter Waves*, vol. 6, K. J. Button, Ed. New York: Academic Press, 1982, pp. 277–343.

[5] G. J. Gibbins, "Improved algorithms for the determination of specific attenuation at sea level by dry air and water vapor in the frequency range 1–350 GHz," *Radio Sci.*, vol. 21, pp. 949–954, Nov.–Dec. 1986.

[6] H. B. Wallace, "Millimeter-wave propagation measurements at the ballistic research laboratory," Proc. SPIE, Vol. 305, Atmospheric Effects on Electro-Optics, Infrared and Millimeter Wave Systems Performance, R. B. Gomez (ed.), San Diego, pp. 224–231, Aug. 1981.

[7] V. J. Falcone, Jr. and L. W. Abreu, "Atmospheric attenuation at millimeter and submillimeter waves," in *IEEE EASCON-79* Conf. Rec., vol. 1, pp. 36–41, 1979.

[8] S. D. Robertson, "Targets for microwave radar navigation," *Bell Syst. Tech. J.* vol. 26, pp. 852–869, Oct. 1947.

[9] F. E. Nathanson, *Radar Design Principles*. New York: McGraw-Hill, 1969, pp. 63–67.

[10] J. R. Probert-Jones, "The radar equation in meteorology," *Quart. J. Royal Meteor. Soc.*, vol. 88, pp. 485–495, 1962.

Robert E. McIntosh (S'66–M'67–SM'72–F'85) was born in Hartford, CT. He received the B.S. degree from Worcester Polytechnic Institute in electrical engineering in 1962, the S.M. degree from Harvard University in 1964, and the Ph.D. degree from the University of Iowa in 1967.

He was a member of the technical staff of Bell Telephone Laboratories, Inc., in North Andover, MA, from 1962 until 1965 where he worked in a microwave networks group. In 1967 he joined the Department of Electrical and Computer Engineering at the University of Massachusetts, where he now is a professor. He spent the 1973–1974 academic year as Guest Professor of Experimental Physics at the University of Nijmegen in the Netherlands, and 1980–1981 with the Electromagnetics Research Branch at NASA Langley Research Center. His teaching and research interests are in electromagnetic field theory, microwave engineering, wave propagation, and remote sensing. He received the Senior Faculty Scholarship Award from the College of Engineering Alumni in 1984 and the Department EKN Teaching Award in 1987.

Dr. McIntosh is a recipient of an IEEE Centennial Medal. He was the general chairman of the 1976 International AP-S/URSI Symposium and the 1985 International Geoscience and Remote Sensing Symposium, held in Amherst. He has served on the Administrative Committees of the Geoscience and Remote Sensing Society and the Antennas and Propagation Society and was elected president of GRS-S in 1984 and AP-S in 1985. He received the GRS-S Distinguished Service Award in 1985. He also served as Associate Editor of the IEEE TRANSACTIONS ON ANTENNAS AND PROPAGATION and is currently an Associate Editor of *Radio Science*. As a member of the Technical Activities Board of the IEEE and Commissions B, C, F, and H of the USNC/URSI, he has served on various technical subcommittees. Presently, he is a member of the United States National Committee of URSI and serves the IEEE as a member of the Fellows Committee and the Engineering Research and Development Committee. He is also a member of the American Physical Society, Sigma Xi, Tau Beta Pi, Phi Kappa Phi, and Eta Kappa Nu.

Ram M. Narayanan (S'83) was born in Tambaram, India, on September 25, 1955. He received the B.Tech degree in electrical engineering from the Indian Institute of Technology, Madras, in 1976.

From 1976 to 1983, he was employed as a Research and Development Engineer at Bharat Electronics Limited, Ghaziabad, India, where he was involved in the development of microwave troposcatter communication equipment and in the indigenization of various MIC subassemblies used in the equipment. He joined the Microwave Remote Sensing Laboratory at the University of Massachusetts, Amherst, in 1983 as a Research Assistant, where he is currently working toward the Ph.D. degree. His current research interests are in the areas of electromagnetic scattering and propagation at millimeter wavelengths. He is also presently teaching an undergraduate course at the University of Massachusetts.

Mr. Narayanan is a student member of AGU and ASPRS.

✠

James B. Mead (S'86) was born in Morristown, NJ, on December 31, 1958. He received the B.S.E.E. degree from the University of Virginia in 1981.

From 1981 to 1986, he was with the RF Engineering Department of Singer Kearfott Division in Wayne, NJ, designing microstrip antennas for Doppler navigation systems. In June 1986, he joined the Microwave Remote Sensing Laboratory at the University of Massachusetts, Amherst, where he is currently pursuing the Ph.D. degree. He is presently working on microwave and millimeter-wavelength radars and radiometers for atmospheric research.

✠

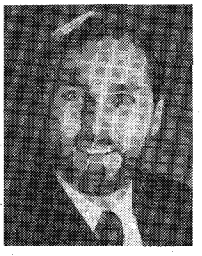

Daniel H. Schaubert received the B.S., M.S., and Ph.D. degrees in electrical engineering from the University of Illinois.

He is currently Associate Professor of Electrical and Computer Engineering at the University of Massachusetts. His current research interests include antenna design and analysis and numerical solution of electromagnetic scattering problems. He is particularly interested in problems involving dielectric media and applications to monolithic integrated circuits at microwave and millimeter-wave frequencies, and in radiation of short-duration pulses. From 1974 to 1980, Dr. Schaubert was a senior R&D engineer at Harry Diamond Laboratories, Adelphi, MD. From 1980 to 1982 he was a project engineer and program manager at the Bureau of Radiological Health, Rockville, MD.

Dr. Schaubert is active in the IEEE Antennas and Propagation Society, having served as a member of the AdCom and as chairman of the Membership Committee and the Washington, DC Chapter. He was editor of the *AP-S Newsletter* and is currently Secretary–Treasurer of the society. He has served on the Technical Review Committee for the Joint Services Electronics Program and several ad hoc panels and review boards, and he is a member of Eta Kappa Nu and Tau Beta Pi.